THE FASEB JOURNAL • RESEARCH • www.fasebj.org

Renal progenitor cells revert LPS-induced endothelial-to-mesenchymal transition by secreting CXCL6, SAA4, and BPIFA2 antiseptic peptides

Fabio Sallustio,[*,†,1,2] Alessandra Stasi,[†,1] Claudia Curci,[*,†] Chiara Divella,[†] Angela Picerno,[†] Rossana Franzin,[†] Giuseppe De Palma,[‡] Monica Rutigliano,[§] Giuseppe Lucarelli,[§] Michele Battaglia,[§] Francesco Staffieri,[¶] Antonio Crovace,[¶] Giovanni Battista Pertosa,[†] Giuseppe Castellano,[†] Anna Gallone,[*] and Loreto Gesualdo[†]

[*]Department of Basic Medical Sciences, Neuroscience and Sense Organs, [†]Nephrology, Dialysis, and Transplantation Unit, Department of Emergency and Organ Transplantation, [§]Urology, Andrology, and Renal Transplantation Unit, Department of Emergency and Organ Transplantation, and [¶]Veterinary Surgery Unit, Department of Emergency and Organ Transplantation, University of Bari Aldo Moro, Bari, Italy; and [‡]Institutional Biobank, Experimental Oncology and Biobank Management Unit, Istituto di Ricovero e Cura a Carattere Scientifico (IRCCS) Istituto Tumori Giovanni Paolo II, Bari, Italy

ABSTRACT: Endothelial dysfunction is a hallmark of LPS-induced acute kidney injury (AKI). Endothelial cells (ECs) acquired a fibroblast-like phenotype and contributed to myofibroblast generation through the endothelial-to-mesenchymal transition (EndMT) process. Of note, human adult renal stem/progenitor cells (ARPCs) enhance the tubular regenerative mechanism during AKI but little is known about their effects on ECs. Following LPS exposure, ECs proliferated, decreased EC markers CD31 and vascular endothelial cadherin, and up-regulated myofibroblast markers, collagen I, and vimentin. The coculture with ARPCs normalized the EC proliferation rate and abrogated the LPS-induced EndMT. The gene expression analysis showed that most of the genes modulated in LPS-stimulated ARPCs belong to cell activation and defense response pathways. We showed that the ARPC-specific antifibrotic effect is exerted by the secretion of CXCL6, SAA4, and BPIFA2 produced after the anaphylatoxin stimulation. Next, we investigated the molecular signaling that underlies the ARPC protective mechanism and found that renal progenitors diverge from differentiated tubular cells and ECs in myeloid differentiation primary response 88–independent pathway activation. Finally, in a swine model of LPS-induced AKI, we observed that activated ARPCs secreted CXCL6, SAA4, and BPIFA2 as a defense response. These data open new perspectives on the treatment of both sepsis- and endotoxemia-induced AKI, suggesting an underestimated role of ARPCs in preventing endothelial dysfunction and novel strategies to protect the endothelial compartment and promote kidney repair.—Sallustio, F., Stasi, A., Curci, C., Divella, C., Picerno, A., Franzin, R., De Palma, G., Rutigliano, M., Lucarelli, G., Battaglia, M., Staffieri, F., Crovace, A., Pertosa, G. B., Castellano, G., Gallone, A., Gesualdo, L. Renal progenitor cells revert LPS-induced endothelial-to-mesenchymal transition by secreting CXCL6, SAA4, and BPIFA2 antiseptic peptides. FASEB J. 33, 10753–10766 (2019). www.fasebj.org

KEY WORDS: endothelial dysfunction · stem cells · antifibrotic effects

Sepsis represents a very relevant problem in critically ill patients and is the leading cause of acute kidney injury (AKI) (1). Despite relevant therapeutic advances, AKI still remains associated with an increased risk for progression to chronic kidney disease and death (2). Gram-negative bacteria and their cell-wall component LPS are frequently involved in the pathogenesis of both sepsis and endotoxemia-induced AKI (3, 4).

Among the several changes encountered in sepsis, endothelial dysfunction is the major complication (5–7). Endothelial cells (ECs) become dysfunctional, switch from a quiescent to an activated state (8), and contribute to the generation of a certain percentage of renal fibroblasts through the endothelial-to-mesenchymal transition (EndMT) (3, 8, 9). This process allows ECs to acquire a mesenchymal phenotype with an overproduction of profibrotic factors contributing to fibrosis and chronic kidney disease (3, 9). Because EndMT contributes to the accumulation of activated fibroblasts and myofibroblasts in renal fibrosis, targeting EndMT might have therapeutic potential.

ABBREVIATIONS: α-SMA, α-smooth muscle actin; AKI, acute kidney injury; Akt, protein kinase B; ARPC, adult renal stem/progenitor cell; EC, endothelial cell; EndMT, endothelial-to-mesenchymal transition; FACS, fluorescence-activated cell sorting; GSEA, gene set enrichment analysis; IRF3, IFN regulatory factor 3; MYD88, myeloid differentiation primary response 88; RPTEC, renal proximal tubular epithelial cell; TRIF, TIR domain-containing adapter-inducing IFN-β; VE, vascular endothelial

[1] These authors contributed equally to this work.

[2] Correspondence: Department of Basic Medical Sciences, Neuroscience and Sense Organs, University of Bari "Aldo Moro," Piazza G. Cesare, 11 70124 Bari, Italy. E-mail: fabio.sallustio@uniba.it

doi: 10.1096/fj.201900351R

This article includes supplemental data. Please visit *http://www.fasebj.org* to obtain this information.

Dysfunctional ECs lead to altered vascular tone, intravascular coagulation, leukocyte adhesion and trafficking, and glomerular microthrombi (10–12).

LPS activate ECs and renal tubular cells through TLR4, LPS binding protein, myeloid differentiation protein-2, and CD14 complex (13–15). LPS binding protein and CD14 facilitate the transfer of LPS to the receptor complex formed by TLR4 and myeloid differentiation protein-2 adaptor protein (16, 17), which consequently leads to the stimulation of both myeloid differentiation primary response 88 (MyD88)-dependent and MyD88-independent pathways. The MyD88-dependent pathway regulates the release of proinflammatory cytokines. Otherwise, the MyD88-independent pathway induces expression of IFN-inducible genes through activation of the transcription factor IFN regulatory factor 3 (IRF3), which enhances anti-inflammatory genes (13).

Of note, human adult renal stem/progenitor cells (ARPCs) enhance the tubular regenerative mechanism during AKI and could be considered an alternative approach in the treatment of kidney diseases for their multipotent differentiation ability and for their reparative properties (18–22). Renal progenitors can induce the renewal of renal tissue, directly regenerating damaged cells (23) and also repairing physical or chemical damage in renal tubular cells through paracrine effects following TLR2-mediated activation (18, 19).

In this study, we investigated whether ARPCs interact with ECs and whether renal progenitors affect the EndMT process induced by LPS. Moreover, we studied the molecules and the signal transduction by which ARPCs influence the endothelial compartment.

MATERIALS AND METHODS

Coculture experiments

We isolated and characterized human ARPCs as previously described in refs. 18, 19, and 24. Human renal proximal tubular epithelial cell (RPTEC)–TERT1 and human umbilical vein EC lines were purchased from American Type Culture Collection (ATCC-LGC Standards, Sesto San Giovanni, Italy). ARPCs, RPTECs, and ECs were maintained in their recommended media: endothelial cell growth medium (Lonza, Basel, Switzerland) supplemented with 20% fetal bovine serum, Prox-Up (EverCyte GmbH, Vienna, Austria), and EndGro (Merck Millipore, Darmstadt, Germany), respectively. EC and RPTEC media were serum-free, and all EC or RPTEC and ARPC cocultures were performed in EC or RPTEC media.

For *in vitro* experiments, cells were plated at a density of 10,000 cells/cm^2, and 48 h later, they were incubated in medium alone or stimulated with LPS 4 μg/ml (MilliporeSigma, Burlington, MA, USA), BPIFA2 4 ng/ml (Sino Biological, Beijing, China), SAA4 20 ng/ml, CXCL6 2.5 ng/ml, or SAA2 5 ng/ml (OriGene, Rockville, MD). For coculture experiments, ARPCs were seeded on the top of 0.4-mm-thick polycarbonate Transwell plates (Costar; Corning, Corning, NY, USA) at a density of 8000 cells/cm^2 and were used for cocultures after 48 h. For TLR4 and TLR2 inhibition assays, 4 μg/ml mouse monoclonal anti-TLR4 (Abcam, Cambridge, United Kingdom) or 0.4 μg/ml mouse monoclonal anti-TLR2 (Santa Cruz Biotechnology, Dallas, TX, USA) (18) were respectively preincubated alone for 1 h before coculture with ECs and then washed out.

Cell growth determination kit

ECs were stimulated *in vitro* with LPS (4 μg/ml) for 48 h and cocultured with ARPCs for 24 h. At the end of the coculture, ECs were plated in flat-bottomed 96-well plates at a density of 2×10^4 cells per well in 100 μl complete culture medium.

EC proliferation was evaluated by measuring the activity of living cells *via* mitochondrial dehydrogenase activity by 3-(4,5-dimethylthiazol-2-yl)-2,5-diphenyl tetrazolium bromide or methylthiazol tetrazolium by a colorimetric immunoassay according to the manufacturer's guidelines (MilliporeSigma).

The absorbances obtained were compared with an appropriate absorbance-cell number curve. A total of 3 independent experiments were performed.

Gene expression

Total RNA concentration and integrity were assessed using a Nanodrop Spectrophotometer ND-1000 (Thermo Fisher Scientific, Waltham, MA, USA) and an Agilent 2100 Bioanalyzer (Agilent Technologies, Santa Clara, CA, USA), respectively. For transcriptomic profiling of ARPCs, labeled cRNA was generated using the Low Input Quick Amp Labeling Kit (Agilent Technologies) from RNA samples. Labeled cRNA was obtained according to the manufacturer's protocols (Agilent Technologies). Data extraction was performed using Agilent Feature Extraction software (v.10.7.3).

Results of the microarray experiments are available in the National Center for Biotechnology Information Gene Expression Omnibus database (accession no. GSE116849; *https://www.ncbi.nlm.nih.gov/geo/*).

Microarray statistical analyses were performed by Genespring GX 11.0 software (Agilent Technologies). Identification of genes differentially expressed between ARPCs and ARPCs stimulated with LPS was carried out with the false-discovery rate method of Storey bootstrapping (25), and gene probe sets were filtered on the basis of the q value cutoff of 0.05 and fold change. The fold change filter was set to 2-fold in each comparison. Only genes that were significantly (adjusted value $P < 0.05$ and fold change >2) modulated were considered for further analysis.

Moreover, gene set enrichment analysis (GSEA) was performed in pairwise comparisons of ARPCs and ARPCs stimulated with LPS. GSEA analyzes gene expression data and determines whether a particular set of genes is over- or under-represented in the compared samples (19). C2 curated gene sets from the Broad Institute (*http://www.broad.mit.edu/index.html*), based on prior biologic knowledge, were used for the analysis. Genes were identified and annotated by Entrez Gene (National Center for Biotechnology Information, Bethesda, MD, USA, (*http://www.ncbi.nlm.nih.gov/gene*). The significance of differential expression, as determined by the enrichment analysis, was recalculated 1000 times. A corrected P value was obtained from the analysis using the false discovery rate q value correction. Based on this correction, the cutoff for significance was established at a value $P < 0.05$.

Flow cytometry analysis

The expression of TLR4 on ECs, ARPCs, and RPTECs surfaces was analyzed using unconjugated mouse monoclonal anti-TLR4 (Abcam) labeled with secondary antibody Alexa Fluor 488 (Thermo Fisher Scientific).

EC phenotype was analyzed by surface staining using allophycocyanin-conjugated anti-CD31 (Miltenyi Biotec, Bergisch Gladbach, Germany), phycoerythrin-conjugated anti–vascular endothelial (VE) cadherin (Miltenyi Biotec) and FITC-conjugated anti–*N*-cadherin (BD Biosciences, Franklin Lakes, NJ, USA) and

intracellular staining using *PE*-conjugated anti-vimentin (Miltenyi Biotec) and FITC-conjugated anti–collagen I (Millimark; MilliporeSigma).

At the end of *in vitro* stimulations, the cells were washed twice with PBS and removed with PBS-EDTA 2 mM and trypsin × 0.001. For surface staining, cells were resuspended in flow cytometry [fluorescence-activated cell sorting (FACS)] buffer (PBS pH 7.2, 0.2% bovine serum albumin, and 0.02% sodium azide) and incubated with FcR blocking reagent (Miltenyi Biotec) for 10 min at room temperature. After blocking incubation, surface markers were added for 20 min at 4°C. The unconjugated primary antibody was added for 25 min at 4°C, and then cells were washed and labeled with secondary antibody for 25 min at 4°C. Then, cells were washed with the FACS buffer and resuspended in each tube with 500 μl of FACS buffer for FACS analysis.

Intracellular staining was preceded by fixation and permeabilization with IntraPrep Kit (Instrumentation Laboratory, Bedford, MA, USA) before continuing with conjugated antibody staining. Finally, cells were washed twice and resuspended in FACS buffer for acquisition.

Data were obtained by using an FC500 flow cytometer (Beckman Coulter, Brea, CA, USA) and analyzed with Kaluza software (Beckman Coulter, Brea, CA, USA). The area of positivity was determined by using an isotype-matched mAb, and in total, 10^4 events for each sample were acquired. A total of 3 independent experiments were performed.

RNA extraction and real-time PCR analysis

Total RNA was isolated with RNeasy Mini Kit (Qiagen, Hilden, Germany) according to the manufacturer's instructions and quantified by NanoDrop ND-1000 Spectrophotometer (Thermo Fisher Scientific). Its quality was assessed with electrophoresis on the agarose gel (1%). Total RNA (500 μg) was used in an reverse transcription reaction by using the iScript cDNA Synthesis Kit (Bio-Rad, Hercules, CA, USA) according to the manufacturer's instructions. Real-time quantitative PCR was performed on an iCycler Thermal Cycler (Bio-Rad) by using SAA4, SAA2, CXCL6, and BPIFA2 primers (Integrated DNA Technologies, Coralville, IA, USA) in combination with SYBR Green Master Mix (Bio-Rad). The relative amounts of mRNA were normalized to β-actin mRNA as the housekeeping gene. Data were analyzed using the $\Delta\Delta C_t$ method. Primer sequences for these genes are shown in Supplemental Table S1.

ELISA

Supernatants were collected from ECs cultured alone or in the presence of LPS 4 μg/ml for 48 h and ARPCs cultured alone or in the presence of LPS 4 μg/ml for 48 h, and ECs cocultured with ARPCs alone or in presence of LPS 4 μg/ml sera were collected from all animals.

BPIFA2, CXCL6, SAA2, and SAA4 were measured by ELISA using commercially available kits from MyBioSource (San Diego, CA, USA), Elabscience (Houston, TX, USA), and R&D Systems (Minneapolis, MN, USA).

Animal model

The experimental model of endotoxemia was performed in domestic pigs at the Section of Veterinary Clinics and Animal Production, Department of Emergency and Organ Transplantation, University of Bari Aldo Moro after approval by the Ethical Committee of the Italian Ministry of Education, University and Research (MIUR), Protocol 823/2016-PR. Animals were introduced 1 wk before the initiation in order to acclimatize according to the standard guidelines of care for experimental animals. The animals were homogeneous in body weight (45–55 kg) and age (6 mo) and without signs of clinical disease. Overnight food removal with free access to water until premedication was expected in all cases. All animals were premedicated with an intramuscular mixture injection of tiletamine and zolazepam 4 mg/kg (Zoletil 100; Virbac, Carros, France) and atropine 0.04 mg/kg (atropine sulfate 0.1% MilliporeSigma) and 2 μg/kg of dexmedetomidine (Dexdomitor 0.5 mg/ml; Orion Corp., Espoo, Finland). After a satisfactory level of sedation was achieved, 1 of the auricular veins was accessed using a 20-gauge catheter for the administration of fluids and drugs. Animals were induced using 5 mg/kg propofol (Proposure 10 mg/ml, i.v.; Merial, Lyon, France) intubated with an orotracheal cuffed tube, and then connected to the anesthetic circuit for the maintenance of anesthesia with isoflurane (Isoba; Schering-Plough, Kenilworth, NJ, USA) in pure oxygen. All pigs received a constant rate infusion of dexmedetomidine at 1 μg/kg/h for the entire duration of the experiment and were maintained in spontaneous breathing. The depth of anesthesia was considered satisfactory when the palpebral reflex was absent, the eye had a ventromedial position, the mandibular tone was attenuated, and spontaneous movements were limited. However, the end point was to guarantee immobility of the animals and simulate to the greatest possible extent a physiologic state of sleep. Once the anesthetic plan was stabilized, an 18-gauge catheter was placed to either an auricular or a femoral artery, and through a dedicated transducer, all pigs were connected to the pressure recording analytical method monitor for the systemic hemodynamic monitoring.

A double-lumen catheter (7 Fr × 8 in central venous catheter; Arrow International, Cleveland, OH, USA) was introduced under ultrasonographic guidance (11 MHz linear array probe, ProSeries; General Electric, Boston, MA, USA) to the jugular vein and was destined for the LPS and drug administration. All pigs were catheterized with a Foley catheter Fr. size 10 connected to a urine collection bag for the monitoring of urine production.

All the parameters were registered on a data sheet by an unaware operator every 30 min. Ventilation parameters (Datex Ohmeda S/5; General Electric) included respiratory rate (breaths/min), end-expired CO_2 (mmHg), capillary oxygen hemoglobin saturation (%) and peak airway pressure (cmH_2O). Physiologic parameters included body temperature (°C), fluid intake (ml/h), and urine output (ml/kg/h) and were clinically evaluated by the dedicated operator. Hemodynamic monitoring (pressure recording analytical method) included heart rate (beats/min), systolic arterial pressure (mmHg), mean arterial pressure (mmHg), diastolic arterial pressure (mmHg), carbon monoxide (L/min), confidence interval ($L/min/m^2$), and systemic vascular resistance ($dyn{\cdot}s/cm^5$). All hemodynamic data were also automatically registered every 30 s and then transferred thanks to dedicated software on a personal computer allowing for better posterior analysis.

The induction of sepsis was performed in all groups using 300 μg/kg of LPS membrane of *Escherichia coli* diluted in 10 ml of saline solution as previously described by us (3). The LPS injection was administered ~15 min after the stabilization of the anesthetic plan and infused over 30 min. At h 24, the surviving pigs were euthanized using an overdose of intravenous propofol immediately followed by 10 ml i.v. of an oversaturated potassium chloride solution (2 mEq/ml; Galenica Senese, Monteroni d'Arbia, Italy). Kidneys were harvested, and a portion was fixed in buffered formalin (4%) for 12 h and embedded in paraffin by using standard procedures.

Urine samples were collected from all animals, and urinary output was measured and recorded every hour. Swine sera were collected at h 0, at intermediate time points, and at h 24 from an arterial blood catheter. Renal function was measured by creatinine measurements and histologic analysis.

Histologic staining

Tissue samples were processed for routine histologic staining [hematoxylin and eosin, periodic acid-Schiff, silver methenamine, Masson's trichrome, and Sirus red/fast green (MilliporeSigma)].

Digital slides were then acquired by the Aperio ScanScope CS2 device (Aperio, Vista, CA, USA). To characterize the possible development of renal fibrosis, we quantified the green-stained area of Masson's trichrome staining using Adobe Photoshop software (Adobe, San Jose, CA, USA) and expressed it as positive pixel/total pixel by 2 independent observers blinded to the origin of the slides.

Confocal laser scanning microscopy

Swine paraffin-embedded renal sections were stained or double stained for CD133 (Abcam), BPIFA2 (Novus Biologicals, Centennial, CO, USA), SAA4, and CXCL6 (Thermo Fisher Scientific). All the antibodies crossreact with pig tissue. Tissue sections were deparaffinized through xylene and alcohol and underwent epitope retrieval through 3 microwave (750 W) cycles of 5 min in citrate buffer (pH = 6). Then, they were incubated with specific blocking solution, primary antibodies [rabbit polyclonal anti-CD133 1:100, rabbit polyclonal anti-SAA4 1:30, rabbit polyclonal anti-CXCL6 1:50, mouse monoclonal anti-BPIFA2, mouse monoclonal anti–α-smooth muscle actin (α-SMA) 1:100, and rabbit polyclonal anti-CD31 1:30] and the corresponding secondary antibodies (Alexa Fluor 555 goat anti-rabbit; Alexa Fluor 488 goat anti-rabbit, and Alexa Fluor 488 goat anti-mouse; Thermo Fisher Scientific). All sections were counterstained with TO-PRO-3 (Thermo Fisher Scientific) and mounted with fluoromount. Negative controls were prepared by omitting the primary antibody.

Image acquisition was performed with the confocal microscope Leica TCS SP8 (Leica Microsystems, Wetzlar, Germany). The number of $CD31^+/\alpha\text{-}SMA^+$ cells was evaluated in $\geq$10 high-power fields (HPFs) ($\times$630)/section by 2 independent observers blinded to the origin of the slides. In the final counts, there was not interobserver variability >20%.

Statistical analysis

For renal function measurements and quantitation of $CD31^+/\alpha\text{-}SMA^+$ cells in renal tissue, data were expressed as medians ± interquartile range and compared with a Mann-Whitney *U* test. Statistical analysis was performed using the Student's *t* test or ANOVA, as appropriate. A value of $P < 0.05$ was considered significant. Data are expressed as means ± SEM.

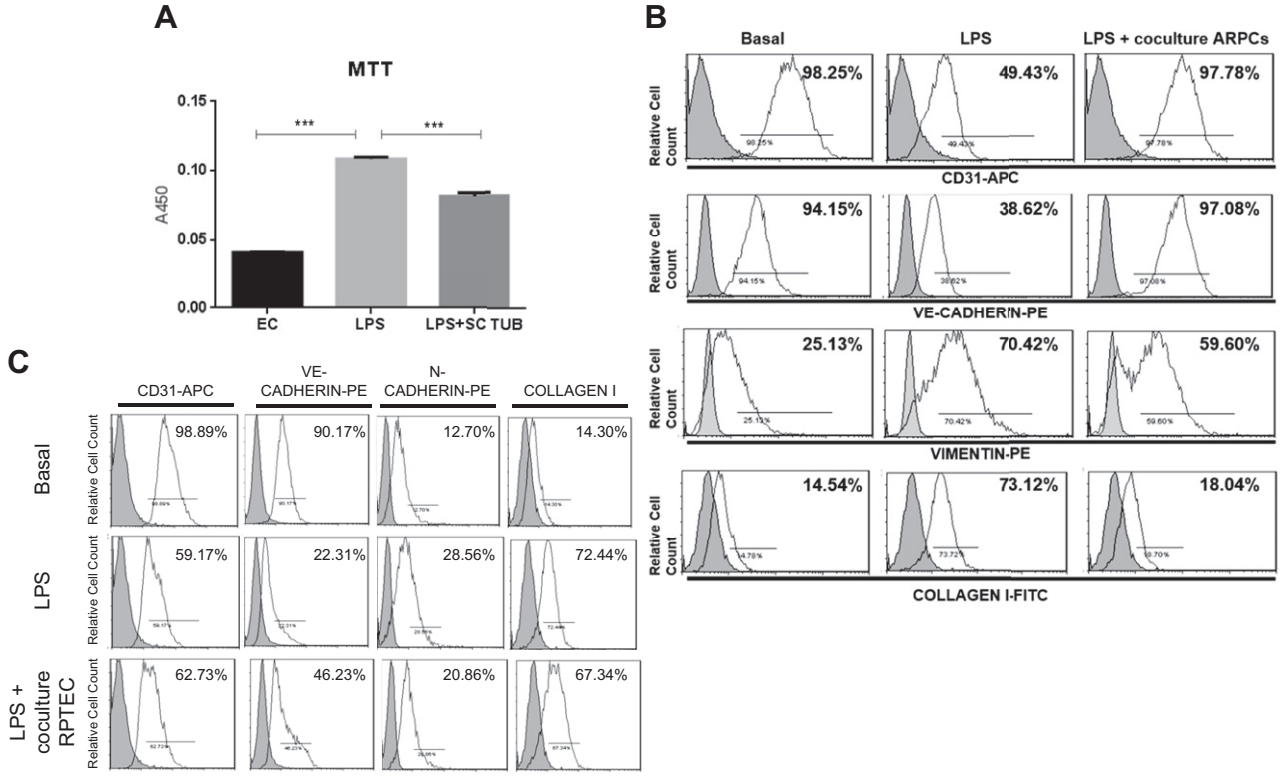

Figure 1. ARPCs normalized EC proliferation rate and abrogated LPS-induced EndMT. *A*) EC proliferation rate was evaluated by the methylthiazol tetrazolium (MTT) test. After 48 h of LPS stimulation, EC proliferated. In addition, ARPCs in coculture with ECs normalized the endothelial proliferation rate and decreased the cell growth rate after only 24 h of coculture. *B*) ECs were incubated alone or in coculture with ARPCs after LPS stimulation. In ECs alone, flow cytometry analysis showed a significant reduction of specific EC markers CD31 and VE-cadherin and an increased expression of dysfunctional fibroblast markers collagen I and vimentin. In coculture with ARPCs, ECs preserved their phenotype. *C*) RPTEC coculture did not abrogate LPS-induced EndMT. After LPS stimulation, ECs were incubated alone or in coculture with RPTECs. In ECs alone, flow cytometry analysis showed a significant reduction of specific EC markers and an increased expression of dysfunctional fibroblast markers. RPTEC coculture did not preserve endothelial phenotype. APC, allophycocyanin; ARPC, adult renal progenitor cells; PE, phycoerythrin. Results are representative of 5 independent experiments on 5 different cell lines. ***$P \leq 0.001$.

TABLE 1. *Defense response gene set composed of genes modulated by LPS in ARPCs ($q < 0.05$, fold change > 2)*

Gene	EntrezGene identifier	FC (ARPC+LPS *vs.* ARPC)	Log_{FC} (ARPC+LPS *vs.* ARPC)	Description
BPIFA2	140683	8.35	3.06	*Homo sapiens* BPI fold containing family A, member 2, mRNA (NM_080574)
CCL5	6352	6.05	2.60	*H. sapiens* chemokine (C-C motif) ligand 5 transcript variant 1, mRNA (NM_002985)
CXCL6	6372	4.17	2.06	*H. sapiens* chemokine (C-X-C motif) ligand 6, mRNA (NM_002993)
SAA2	6289	3.42	1.77	*H. sapiens* serum amyloid A2, transcript variant 1, mRNA (NM_030754)
CAMK2A	815	3.40	1.77	*H. sapiens* calcium/calmodulin-dependent protein kinase II α, transcript variant 1, mRNA (NM_015981)
CCL25	6370	3.36	1.75	*H. sapiens* chemokine (C-C motif) ligand 25, transcript variant 1, mRNA (NM_005624)
SAA4	6291	2.89	1.53	*H. sapiens* serum amyloid A4, constitutive, mRNA (NM_006512)
MYOM1	8736	2.76	1.46	*H. sapiens* myomesin 1, transcript variant 1, mRNA (NM_003803)
BLK	640	2.49	1.32	*H. sapiens* BLK proto-oncogene, Src family tyrosine kinase, mRNA (NM_001715)
DEFB134	613211	2.24	1.16	*H. sapiens* defensin, β 134, mRNA (NM_001302695)
TNFRSF25	8718	−2.07	−1.05	*H. sapiens* tumor necrosis factor receptor superfamily, member 25, transcript variant 12, mRNA (NM_001039664)
CYSLTR1	10800	−2.08	−1.06	*H. sapiens* cysteinyl leukotriene receptor 1, transcript variant 3, mRNA (NM_006639)
CCL21	6366	−2.13	−1.09	*H. sapiens* chemokine (C-C motif) ligand 21, mRNA (NM_002989)
IL-4	3565	−2.22	−1.15	*H. sapiens* IL-4, transcript variant 1, mRNA (NM_000589)
SPN	6693	−2.29	−1.19	*H. sapiens* sialophorin, transcript variant 1, mRNA (NM_001030288)
ANO6	196527	−2.29	−1.20	*H. sapiens* anoctamin 6, transcript variant 3, mRNA (NM_001142679)
DKKL1	27120	−2.30	−1,20	*H. sapiens* Dickkopf-like 1, transcript variant 1, mRNA (NM_014419)
ITGB1	3688	−2.35	−1,23	Integrin β1 (fibronectin receptor, β polypeptide, antigen CD29; includes MDF2 and MSK12) (ENST00000439974)

(*continued on next page*)

TABLE 1. (*continued*)

Gene	EntrezGene identifier	FC (ARPC+LPS *vs.* ARPC)	Log_{FC} (ARPC+LPS *vs.* ARPC)	Description
ESR2	2100	−2.55	−1.35	*H. sapiens* estrogen receptor 2 (ER β), transcript variant a, mRNA (NM_001437)
LILRB3	11025	−2.57	−1.36	*H. sapiens* leukocyte immunoglobulin-like receptor, subfamily B, member 3, transcript variant 2, mRNA (NM_006864)
IL-5	3567	−2.58	−1.37	*H. sapiens* IL-5, mRNA (NM_000879)
CCL4L2	9560	−2.73	−1.45	*H. sapiens* chemokine (C-C motif) ligand 4-like 2, transcript variant CCL4L2b2, mRNA (NM_001291470)
SIRPB1	10326	−2.80	−1.49	*H. sapiens* signal-regulatory protein β 1, transcript variant 1, mRNA (NM_006065)
RPS6KA5	9252	−3.09	−1.63	Ribosomal protein S6 kinase, 90 kDa, polypeptide 5 (Source :HGNC; Symbol;Acc: HGNC:10434) (ENST00000614987)
TIAL1	7073	−3.12	−1.64	TIA1 cytotoxic granule-associated RNA binding protein-like 1 (Source: HGNC; Symbol;Acc: HGNC:11804) (ENST00000369086)
LILRA1	11024	−3.58	−1.84	*H. sapiens* leukocyte immunoglobulin-like receptor, subfamily A, member 1, transcript variant 1, mRNA (NM_006863)
TNFRSF14	8764	−4.87	−2.28	*H. sapiens* TNF receptor superfamily, member 14, transcript variant 1, mRNA (NM_003820)

Entrez Gene (National Center for Biotechnology Information, Bethesda, MD, USA; *http://www.ncbi.nlm.nih.gov/gene*).

RESULTS

ARPCs can inhibit EndMT and endothelial dysfunction

To study whether ARPCs can affect EndMT, we stimulated ECs with and without 4 μg/ml LPS and cultured them alone or in coculture with ARPCs. We have previously shown that only a small percentage of ECs underwent apoptosis and a significant proliferation was instead described after LPS stimulation in a swine model of LPS-induced AKI (3). Therefore, we analyzed the EC proliferation rate following LPS stimulation in the coculture system, and we observed increased proliferation of ECs after 48 h of stimulation (1.7-fold compared with basal condition; $P < 0.05$). Interestingly, ARPCs in coculture with ECs significantly decreased the EC growth rate, even in the presence of LPS, after only 24 h of coculture (**Fig. 1*A***).

Next, we characterized ARPC effects on LPS-induced EndMT by flow cytometry analysis. Here, we confirmed that LPS induced EndMT, decreasing significantly specific EC markers such as CD31 (67 *vs.* 97% basal; $P = 0.01$) and VE-cadherin (31 *vs.* 96% basal; $P = 0.001$) and up-regulating markers of EC dysfunction such as collagen I (73 *vs.* 14% basal; $P = 0.03$) and vimentin (50.86 *vs.* basal 30%; $P = 0.001$). In addition, ARPCs in coculture with ECs abrogated the LPS-induced EndMT by restoring the high expression of CD31 (95 *vs.* 66% ECs without ARPCs; $P = 0.005$) and VE-cadherin (96 *vs.* 31% ECs without ARPCs; $P = 0.001$) and the low expression of collagen I (18 *vs.* 73% ECs without ARPCs; $P = 0.001$) and vimentin (35 *vs.* 50.86% ECs without ARPCs; $P = 0.03$).

Our data revealed that ARPCs inhibited endothelial dysfunction and restored constitutive endothelial and dysfunctional fibroblastic markers to the basal levels (Fig. 1*B*). This protective effect was specific to ARPCs because the replacement of ARPCs with RPTECs in the

coculture system did not induce the blocking of EndMT (Fig. 1C).

Gene expression screening of ARPC response to LPS

To identify genes activated in ARPCs that could be involved in the reversion of the EndMT process, we performed a genome-wide gene expression screening on the whole transcriptome of ARPCs alone or after 24 h of in presence of LPS. We found that LPS down-regulated most of the genes of ARPCs in coculture (695 genes; $q < 0.05$; fold change >2), and overexpressed 305 genes (**Fig. 2*A***and Supplemental Table S2).

Then, to define whether LPS in ARPCs give rise to a coordinated expression or enrichment in a set of functionally related genes, we performed GSEA, identifying 25 processes differentially regulated during the 24 h of LPS exposure. Among the most significant modulated biologic processes, we found "defense response," "positive regulation of cell communication," "regulation of cell death," and "response to endogenous stimulus" ($q < 0.05$; Supplemental Table S3).

In particular, in the defense response gene set, composed of 10 up-regulated and 17 down-regulated genes (Fig. 2*B* and **Table 1**; $q < 0.05$; fold change >2) specifically involved in damage-limiting biologic processes or preventing or recovering from infection caused by external agents, we found a cluster of 4 up-regulated genes implicated in the systemic septic response: BPIFA2, CXCL6, SAA2, and SAA4.

Validation of the 4 gene signatures

To validate microarray results and to study whether LPS increased CXCL6, SAA2, SAA4, and BPIFA2 expression only in ARPCs or also in other kinds of cells, we validated the 4 genes identified by the microarray studies by RT-PCR on an independent set of ARPCs (**Fig. 3*A***) and also on RPTECs and ECs. The LPS stimulation significantly increased the 4 genes' expression in ARPCs (fold increase of 5.4, 8.5, 5.8, and 3.4 for CXCL6, SAA2, SAA4, and BPIFA2, respectively), whereas it did not increase their expression in RPTECs (Fig. 3*A*, *B*). Interestingly, in ECs, LPS can induce a gene expression increment for CXCL6 but did not augment SAA2 and BPIFA2 mRNA levels (Fig. 3C). The increase in SAA4 transcript is not significant and it is less strong with respect to that in ARPCs. However, the endotoxin-induced a CXCL6 expression gain of 1.5-fold higher in renal progenitors compared with ECs.

ARPCs regulated endothelial dysfunction by secretion of CXCL6, SAA2, SAA4, and BPIFA2 chemokines

Our microarray and quantitative PCR data revealed a significant up-regulation of CXCL6, SAA2, SAA4, and BPIFA2 gene expression in ARPCs. To further validate data and to verify that these transcripts lead effectively to the release of the relative proteins by ARPCS, we performed ELISA assays using supernatants of ARPCs grown alone, ARPCs treated for 48 h with LPS, ECs grown alone, ECs treated for 48 h with LPS, and ECs put in coculture with ARPCs in the presence or absence of LPS (**Fig. 4**).

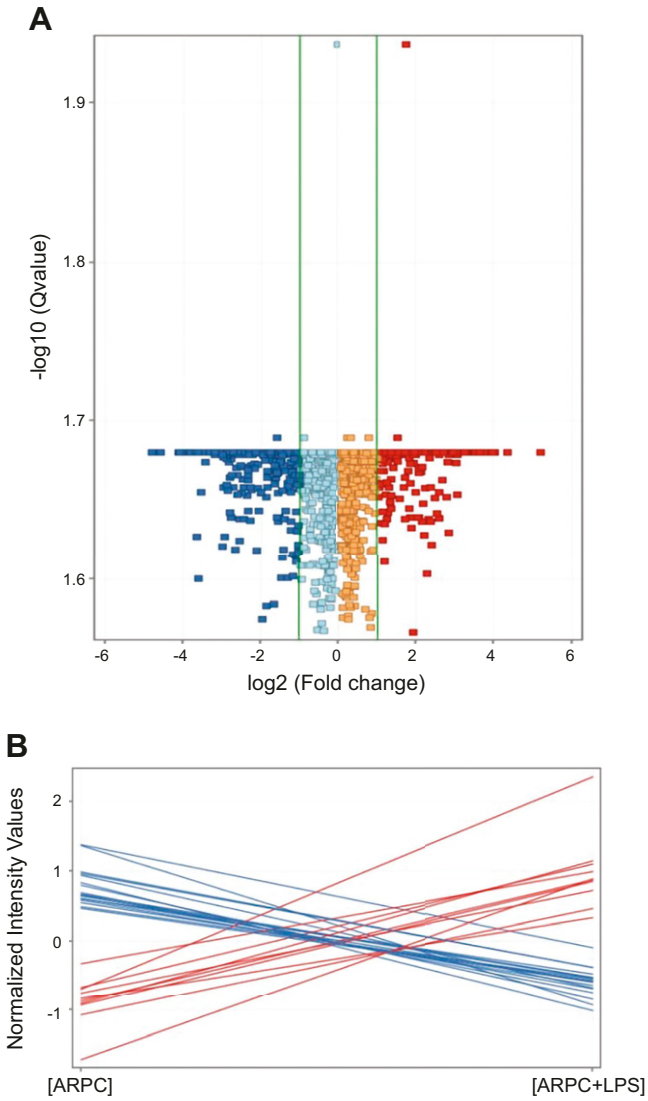

Figure 2. LPS-modulated genes in ARPCs. *A*) Scatter plot showing genes modulated by LPS in ARPCs on the basis of the *q* value cutoff of 0.05 and fold change of 2. LPS down-regulated 695 genes and up-regulated 305 genes of ARPCs. *B*) Profile plot showing the gene set defense response deriving from the gene set enrichment analysis composed of 10 up-regulated and 17 down-regulated genes in ARPCs by LPS with a value of $q < 0.05$ and fold change >2.

We showed that ARPCs expressed these proteins in normal growing conditions and that their expression significantly increased after LPS stimulation.

Moreover, we observed that ECs did not increase the release of these proteins in basal condition or after stimulation with LPS. On the contrary, in the coculture system, in presence of LPS, there was a significant increase in these molecules. Altogether, these results are consistent with the idea that ARPCs specifically secreted this protein cluster in response to LPS, modulating endothelial behavior and phenotype.

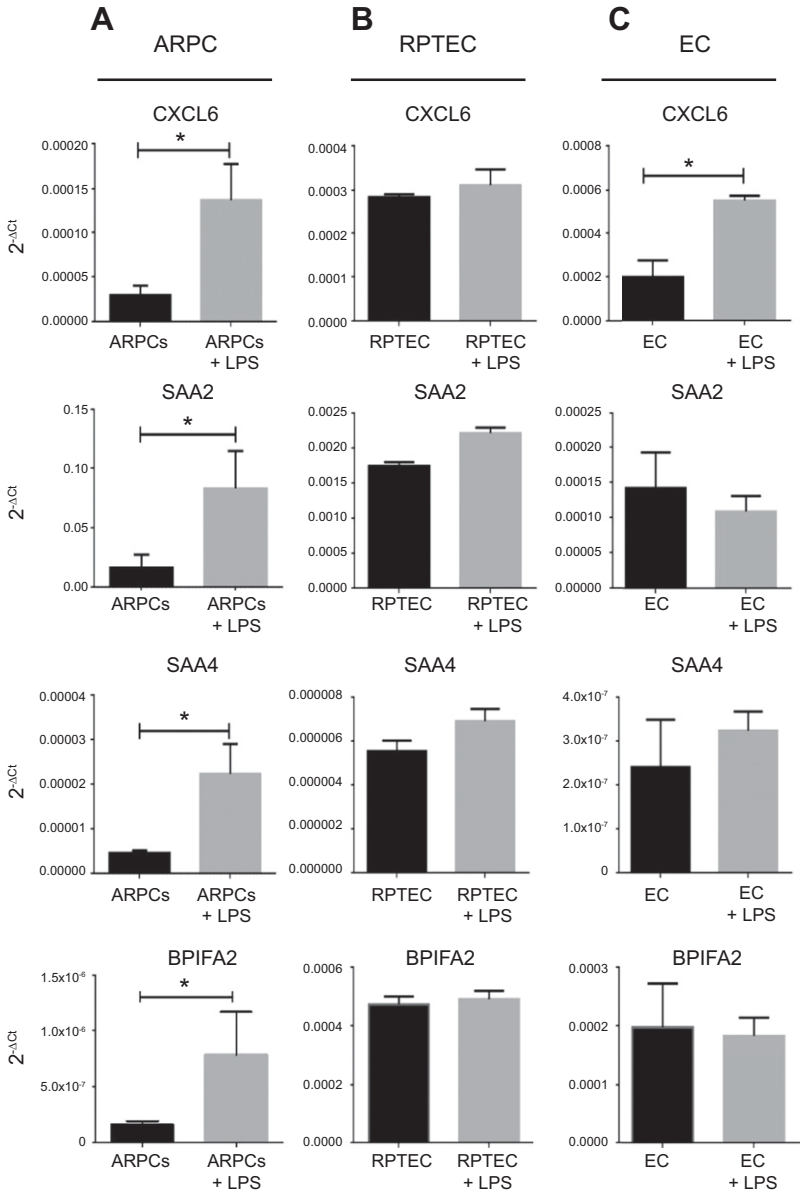

Figure 3. Validation of target genes by real-time PCR. ARPCs (*A*), ECs (*B*), and RPTECs (*C*) were stimulated with LPS for 24 h. The relative expression of CXCL6, SAA2, SAA4, and BPIFA2 was evaluated by real-time PCR. The LPS stimulation significantly increased the 4 genes' expression in ARPCs (*A*), whereas it did not increase their expression in RPTECs (*B*). In ECs, LPS can induce a gene expression increment only for CXCL6 (*C*). Data are expressed as the mean ± SEM of 5 independent experiments on 5 different cell lines. $*P < 0.05$.

CXCL6, SAA4, and BPIFA2 reverted EndMT

We then investigated whether CXCL6, SAA2, SAA4, and BPIFA2 were sufficient to block the EndMT process in the presence of LPS. Simulating the coculture system, after 24 h from LPS stimulation, ECs were treated for 24 h with these factors at the same concentrations found in ELISA measurements and analyzed by FACS (**Fig. 5**).

As expected, LPS induced phenotypic changes in ECs with the acquisition of a myofibroblast phenotype: CD31 and VE-cadherin significantly decreased, and collagen I and vimentin significantly increased. In addition, the identified chemokines, also individually, could preserve endothelial phenotype and counteract the LPS detrimental effects. Weaker results were observed in response to SAA2 for collagen I expression (Fig. 5). This result suggests that SAA2 can not completely stop the EndMT process.

These data suggest that these proteins might interfere with the activation of the endothelial compartment, limiting early fibrosis in sepsis-induced AKI.

LPS-stimulated ARPCs activated the MyD88-independent pathway

We investigated the intracellular signaling activated in ECs, RPTECs, and ARPCs following LPS stimulation. First, we analyzed whether TLR2, expressed on ARPCs, is involved together with TLR4 in the LPS-induced activation of ARPCs. We blocked the TLR2 or the TLR4 in ARPCs by the corresponding specific mAb and cocultured them with ECs. We found that ARPCs pretreated for anti-TLR4 did not revert the LPS-induced EndMT process, confirming the role of TLR4 in sensing the LPS and activating the downstream pathway. In addition, the TLR2 blocking did not lead to any significant functional effect on ARPCs. They abrogated the EndMT process likewise progenitors without any blocking (Supplemental Fig. S1).

Then, we studied whether a different expression of TLR4 (*i.e.*, the LPS receptor) could explain a dissimilar protective role in preventing endothelial dysfunction of ECs, RPTECs, and ARPCs. We found that TLR4 was

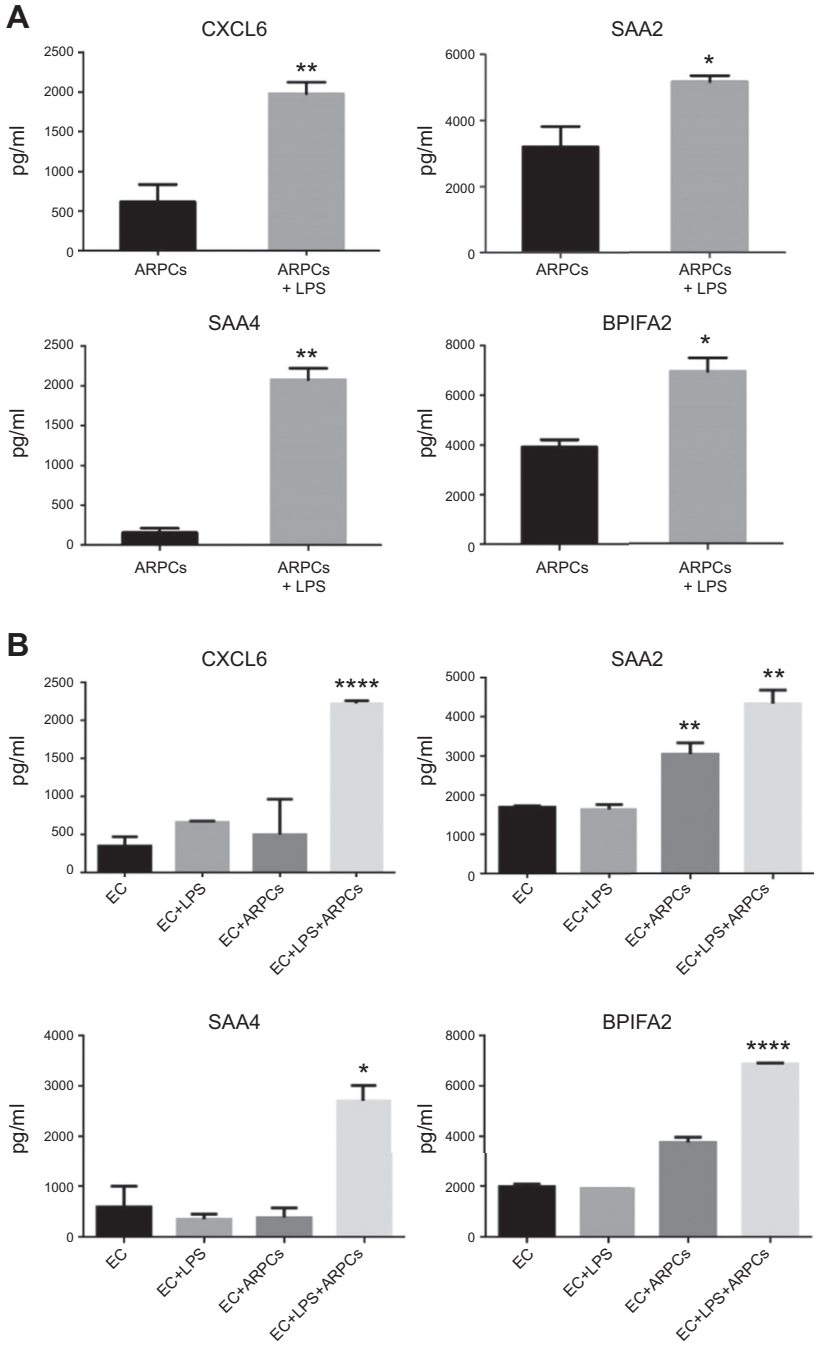

Figure 4. Validation of target genes by ELISA. ELISA for CXCL6, SAA2, SAA4, and BPIFA2 using supernatants of ARPCs or ECs grown alone or in coculture with ARPCs and in the presence or absence of LPS for 48 h. *A*) These proteins were expressed by ARPCs in normal growing conditions and were up-regulated after 48 h of LPS stimulation. *B*) ECs did not increase the release of these proteins in basal conditions or after stimulation with LPS. CXCL6, SAA4, SAA2, and BPIFA2 were secreted only when ARPCs were in coculture with LPS-stimulated ECs. Results represent the mean ± SEM of 5 independent experiments on 5 different cell lines. $^{*}P < 0.05$, $^{**}P < 0.01$, $^{***}P < 0.001$.

expressed almost at the same level as the 3 kinds of cells and that it was not modulated by LPS (**Fig. 6*A***).

TLR4 activates 2 separate signaling pathways: the MyD88-dependent and MyD88-independent pathways. The suppressive effect of ARPCs on endothelial dysfunction was examined with regard to the activation of these 2 signals.

In ARPCs, phosphorylation of IRF3 was found to increase significantly after 30 and 60 min from LPS stimulation compared with basal conditions ($P < 0.01$) in a time-dependent manner. Also, TIR domain-containing adapter-inducing IFN-β (TRIF) was augmented 24 h after TLR4 engagement (Fig. 6*A*). Interestingly, in ECs, IRF3 was expressed but it was not phosphorylated following LPS stimulation and TRIF was not modulated (Fig. 6*B*). Finally, in LPS-stimulated RPTECs, there was no significant phosphorylation of IRF3 and increase of TRIF (Fig. 6*B*). We then studied the activation of the MyD88-dependent pathway through PI3K/protein kinase B (Akt) signaling and observed a significant increase in PI3K phosphorylation only in ECs at 60 min upon LPS stimulation (Fig. 6C). LPS cannot activate the PI3K/Akt signaling in ARPCs or in RPTECs, at least in a short time. Altogether, our data showed that ARPCs differ in MyD88-independent pathway activation following LPS stimulation.

In vivo validation of antiseptic CXCL6, SAA4, and BPIFA2 proteins secreted by ARPCs

To validate also *in vivo* that the 3 proteins were secreted by ARPCs following an endotoxemic event, we used a swine

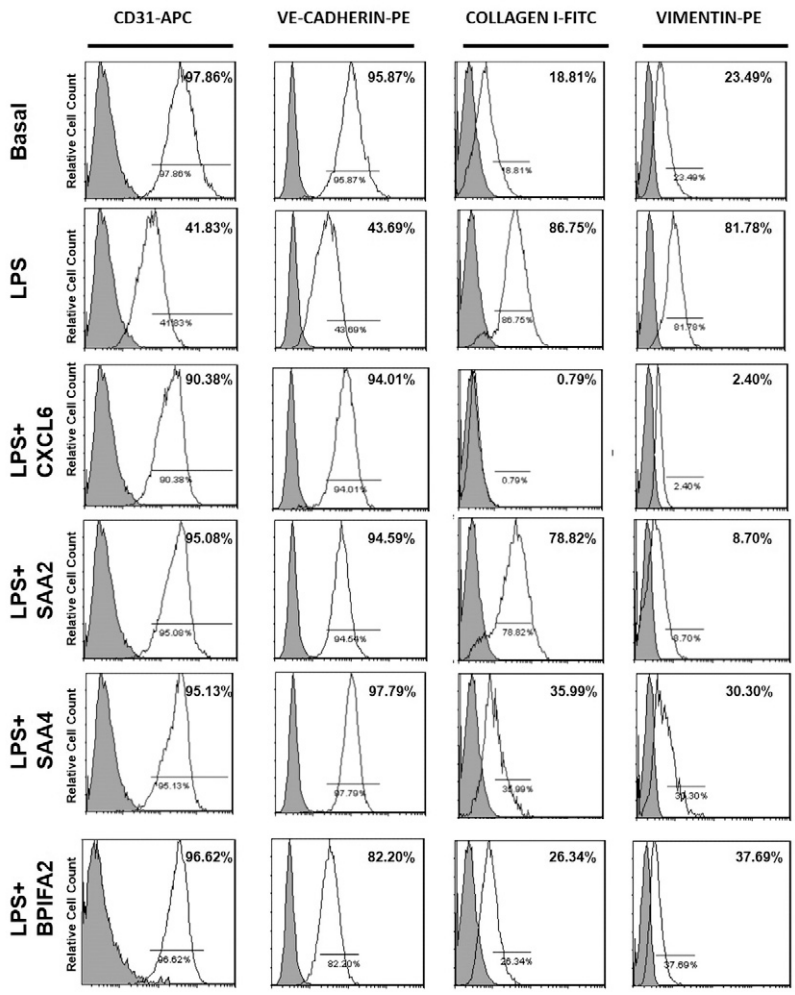

Figure 5. Effects of CXCL6, SAA2, SAA4, and BPIFA2 on ECs *in vitro*. ECs were stimulated by LPS and after 24 h were treated with CXCL6, SAA2, SAA4, or BPIFA2. Endothelial and myofibroblast markers were analyzed by flow cytometry analysis. LPS induced a CD31 and VE-cadherin significant decrease and a collagen I and vimentin significant increase. In addition, CXCL6, SAA2, and BPIFA2 preserved endothelial phenotype and counteracted the LPS detrimental effects. APC, allophycocyanin; PE, phycoerythrin. These data are representative of 3 independent experiments.

model of LPS-induced AKI, in which pigs were infused with 300 μg/kg of LPS. Control pigs received 10 ml of sterile saline solution. As described in results from the previous experimental endotoxemic swine model (3), LPS infusion induced an extensive collagen deposition at tubulointerstitial level, diffuse glomerular thrombi and tubular vacuolization that were not detectable in control animals (Supplemental Fig. S2*A*–*C*). Moreover, we observed that the development of acute fibrosis and inflammation was associated with the increment of serum creatinine (h 24: 2.35 ± 0.475 *vs.* h 0: 1.35 ± 0.375 mg/dl; $P = 0.01$) and the strong decrease of urinary output ($P = 0.001$), suggestive of acute renal dysfunction.

We confirmed that, in the same way of the previous swine model (3), LPS administration leads to a significant increase in $CD31^+/\alpha\text{-}SMA^+$ cells in the interstitium that were rarely detectable in control pigs (Supplemental Fig. S3).

We found that in healthy pig kidneys, ARPCs ($CD133^+$) were normally expressed both in glomeruli and in tubules, and CXCL6, SAA4, and BPIFA2 were not expressed or expressed at low levels (**Fig. 7** and Supplemental Fig. S4). In addition, in endotoxemic pigs, CXCL6, SAA4, and BPIFA2 were highly expressed (especially close to ARPCs); this was even more evident in tubules or glomeruli whose structure was not damaged by LPS (Fig. 7).

We then checked whether these 3 chemokines were expressed and modulated at serum level in our animal model. We found that only BPIFA2 significantly increased after 24 h from LPS infusion (unpublished results).

DISCUSSION

Among the several disorders encountered in sepsis, AKI is the major complication and is mainly characterized by dysfunction of ECs that acquire a myofibroblast phenotype by EndMT, contributing to the renal fibrosis (26–28). Here, we investigated the effects of ARPCs on endothelial dysfunction, and for the first time we found that ARPCs, in addition to their ability to repair damaged renal tubular cells (18) and regenerate renal tubules and glomeruli (23), can also revert the sepsis-induced EndMT process that contributes to the accumulation of activated fibroblasts and myofibroblasts in kidney fibrosis (29–32). In fact, following LPS stimulation, ARPCs restored constitutive endothelial and dysfunctional fibroblastic CD31, VE-cadherin, collagen I, and vimentin markers to basal levels. Moreover, they normalized the EC proliferation rate altered by LPS. We demonstrated that this antifibrotic effect, specific to ARPCs, is exerted by the secretion of CXCL6, SAA2, SAA4, and BPIFA2. Effectively, these

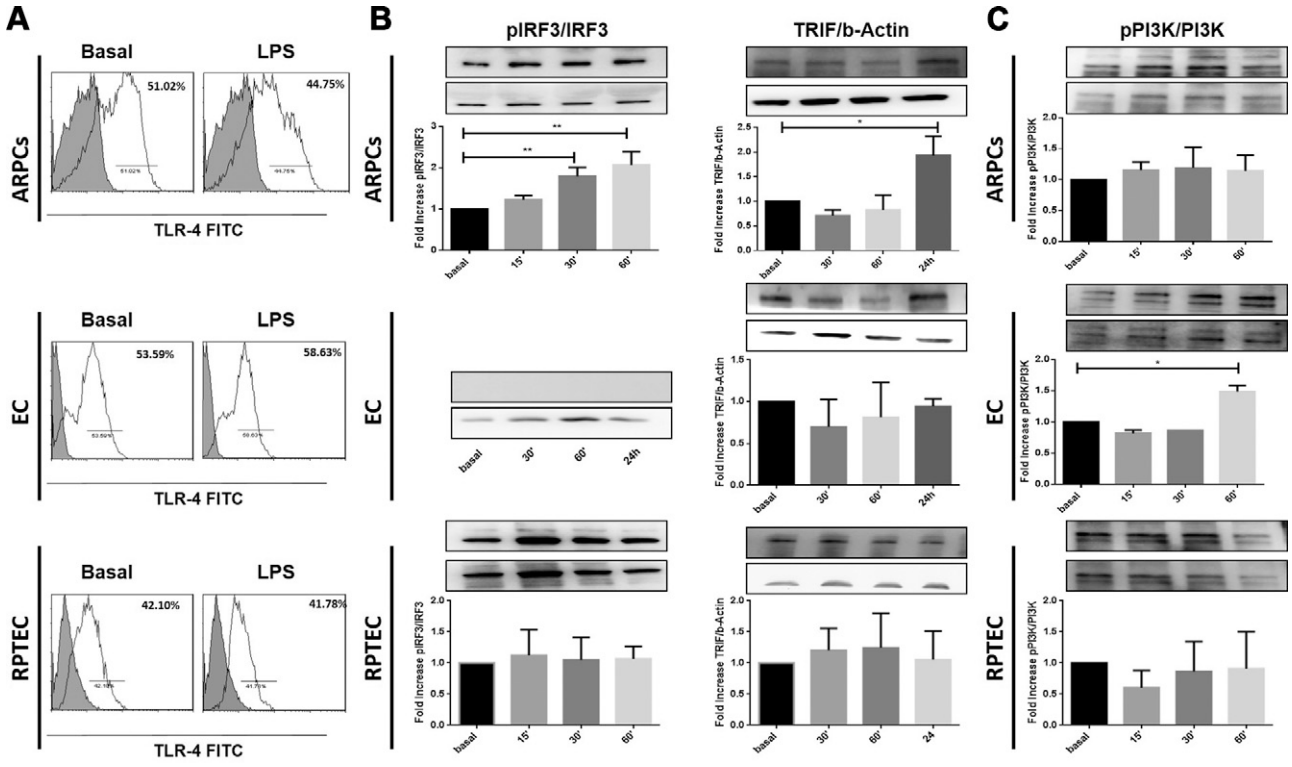

Figure 6. MyD88-independent pathway activation *in vitro*. ARPCs, ECs, and RPTECs were exposed LPS for 48 h. *A*) TLR4 expression was evaluated by FACS analysis. LPS did not modulate TLR4 expression. Results are representative of 3 independent experiments. *B*) ARPCs, ECs, and RPTECs were exposed to LPS for the times indicated and then assayed for IRF3 phosphorylation and TRIF content by Western blotting. Phosphorylated IRF3 (pIRF3) increased significantly in ARPCs after 30 and 60 min from LPS stimulation in a time-dependent manner. TRIF was augmented in ARPCs at 24 h after TLR4 engagement. In ECs, IRF3 was expressed but it was not phosphorylated following LPS stimulation. *C*) ARPCs, ECs, and RPTECs were exposed LPS for the times indicated and then assayed for PI3K phosphorylation by Western blotting. Phosphorylated PI3K (pPI3K) increased in ECs at 60 min upon LPS stimulation. Each blot is representative of 3 experiments. Data are expressed as the mean ± SEM from 3 independent experiments. $^*P < 0.05$, $^{**}P \leq 0.01$.

molecules alone were sufficient to completely block the EndMT process, as demonstrated by our experiments with exogenous synthetic molecule administration. Therefore, once again, ARPCs proved to be capable of producing a precise positive effect through a paracrine mechanism. Additionally, the secreted molecules are different and specific for a particular damage setting; in the case of physical or chemical damage on RPTECs, renal progenitors secreted regenerative molecules such as inhibin-A and decorin (18), whereas in the case of a septic shock, they secreted CXCL6, SAA4, and BPIFA2. The last chemokines belong to an antimicrobial peptide family that attenuates local inflammatory response and decreases the systemic toxicity of endotoxins (33). Granulocyte chemotactic protein 2/CXCL6 is a CXC chemokine expressed by macrophages, ECs, and mesenchymal cells during inflammation and it has strong antibacterial activity against Gram-positive and Gram-negative bacteria by membrane disruption and leakage. It contributes to direct antibacterial activity during localized infection (34). CXCL6 is associated with lung fibrosis (34) and is expressed in ECs (36), as confirmed also by our data. However, for the first time, we found a high expression in response to LPS in renal cells and particularly in ARPCs at a concentration sufficient to block EndMT. In fact, as shown by ELISA experiments, this increase is significant only in ARPCs and not in ECs. In addition, LPS did not induce the CXCL6 increase in RPTECs.

SAA2 and SAA4 belong to the SAA apolipoprotein family, which comprises 4 human gene loci (SAA1, SAA2, SAA3P, and SAA4) (37, 38). In humans, they have consistently been found to be some of the most highly and quickly induced acute phase proteins, with increases in serum concentrations up to 1000-fold (39), even if their function is not very clear (40). SAA2 mRNA has been found to be induced by LPS in mouse kidney proximal and distal convoluted tubule epithelia (41). Recently, SAA2 and SAA4 isoforms have been found to be specific responses to bacterial infection in the liver and lung pigs (42). In this paper, we observed, for the first time, increased expression of SAA4 isoform in endotoxemic renal tissue, in particular at the tubular level in correspondence with ARPC localization. Interestingly, we observed that ARPCs expressed SAA4 protein both *in vivo* and *in vitro*, which influenced endothelial behavior, preventing the EndMT process. Moreover, SAA4 expression was significantly induced by LPS in ARPCs respect to ECs and primary tubular cells. These results suggested that SAA4 is the major inducible SAA isoform in ARPCs, which is able to preserve endothelial phenotype.

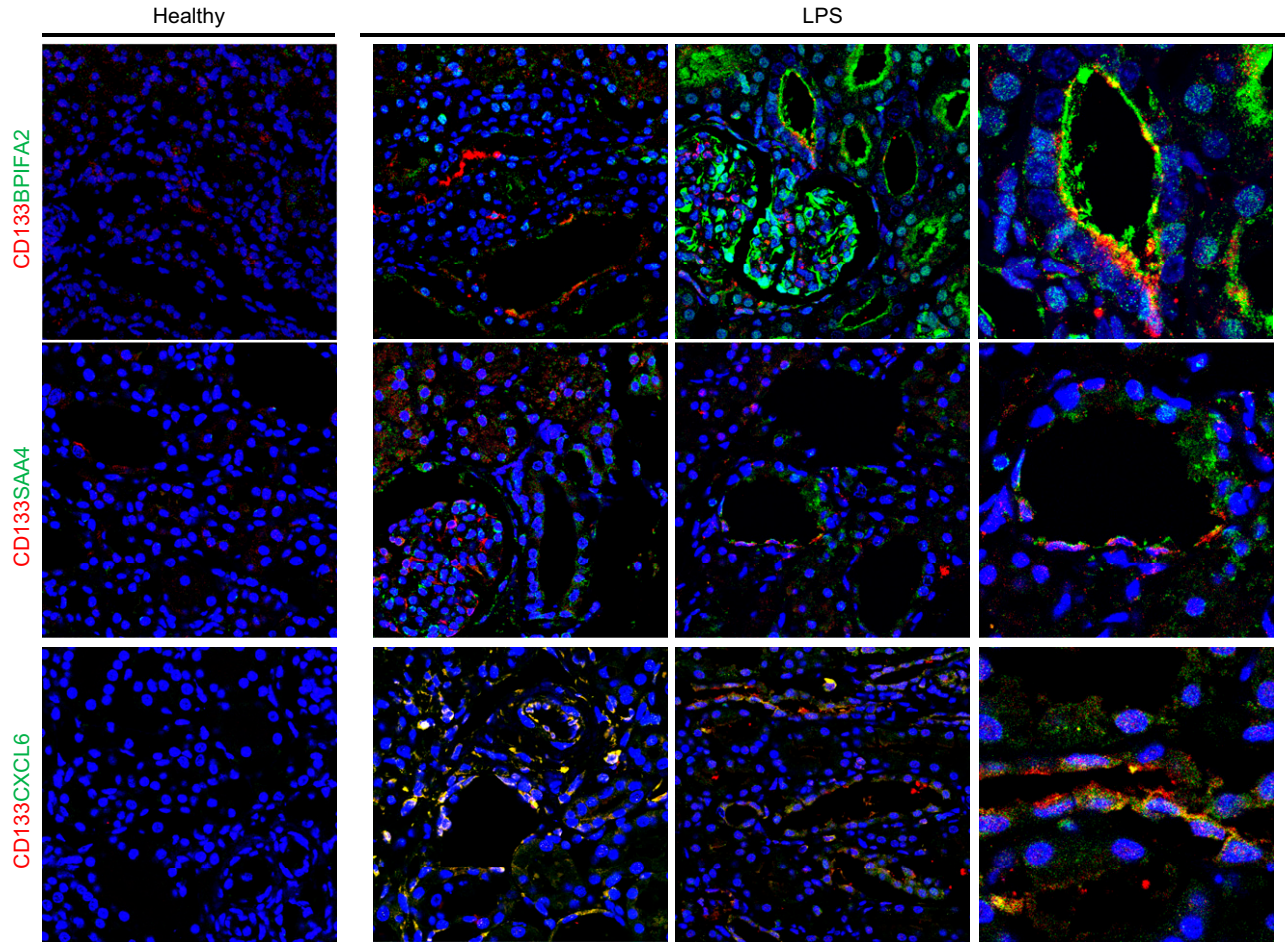

Figure 7. Expression of CXCL6, SAA4, and BPIFA2 by ARPCs *in vivo*. CD133^{+} renal progenitors (red) were normally expressed both in glomeruli and in tubules of healthy pig kidneys (left panels). CXCL6, SAA4, and BPIFA2 (green) were not expressed or expressed at low levels. In addition, in endotoxemic pigs (right panels), CXCL6, SAA4, and BPIFA2 (green) were highly expressed, especially close to ARPCs. Tubules and glomeruli coexpressing CD133 and CXCL6, SAA4, or BPIFA2 resulted in less structural damage by LPS.

BPIFA2 plays a role in the local antibacterial response in nose, mouth, and upper respiratory pathways. The encoded soluble salivary protein binds LPS and inhibits bacterial growth (43–46). Very recently, it has been identified as an early biomarker of AKI, and its plasma levels have been found to be increased during injury induced by LPS (47). Here, we found that in endotoxemic pigs, BPIFA2 was also expressed locally in the renal tubular compartment upon LPS infusion. In particular, we observed that ARPCs preferentially expressed BPIFA2 upon LPS stimulation both *in vivo* and *in vitro* compared with primary tubular cells and ECs. More interestingly, exogenous administration of BPFIA2 completely abrogated the LPS detrimental effects on ECs. Therefore, BPIFA2 is not only a useful biomarker in the prognosis of sepsis-induced AKI but also could contribute to arresting the progression of early fibrosis and the development of chronic kidney disease.

Considering our *in vitro* data about the 4 chemokines overall, it is noteworthy that CXCL6, SAA4, BPIFA2, andSAA2 were secreted by ARPCs selectively following LPS damage. Interestingly, in our animal model of LPS-induced AKI, ARPCs secreted these proteins in the renal parenchyma, plausibly contributing to locally controlling the renal fibrosis induced by LPS. However, further studies should be addressed to investigate the potential antiseptic effects of these molecules at the renal or the systemic level in reducing renal fibrosis induced by LPS. In fact, depending on the specific clinical setting, other chemokines and factors may counterbalance their effects *in vivo*. We also investigated the molecular mechanism of LPS-induced ARPC activation and whether a difference of TLR4 expression in ARPCs, ECs, and RPTECs could determine the different activation in these cells. However, when examined, we did not find any difference in receptor expression between these cells, suggesting that the difference in LPS response leading to ARPC antifibrotic effects may be due to the activation of specific signaling pathways. Effectively, triggering of TLR4 results in the activation of 2 distinct intracellular pathways: the MyD88-dependent and MyD88-independent pathways (48). In particular, the MyD88-independent pathway leads to the phosphorylation of IRF3 upon TIR-domain-containing adaptor-inducing IFN-β (TRIF) activation. The IRF3 activation induces the suppression of proinflammatory cytokines and the promotion of anti-inflammatory or

immunoregulatory cytokines (49). Therefore, we examined the intracellular pathways involved in ARPC activation by LPS conferring on them antifibrotic effects. Interestingly, ARPCs can only activate the MyD88-independent pathway (through IRF3 phosphorylation and increased expression of TRIF) after LPS stimulation; this may explain their peculiar protective effects on the endothelial compartment. In addition, in ECs exclusively, the MyD88-dependent pathway is activated following LPS stimulus. These data are supported by previous studies reporting that the major players involved in eliciting the functional effects of LPS within ECs are activated through the MyD88-dependent pathway, in particular by (PI3K)/Akt signaling, which regulates the balance between cell viability and inflammation (11, 50–52). Considering our data overall, ARPCs diverge from RPTECs and from ECs in MyD88-independent pathway activation following LPS stimulation, at least in the short term. These results indicate that the ARPC protective role on endothelial dysfunction could be mediated by the MyD88-independent pathway.

In summary, we demonstrated for the first time that ARPCs can preserve endothelial phenotype by preventing the development of the LPS-induced EndMT process. We identified the secretion of CXCL6, SAA4, and BPIFA2 antiseptic peptides as the principal mechanism that can counteract the effect of LPS in our model. The peculiar ARPC protective and antifibrotic effects on endothelial compartment may be explained by the selective activation of the MyD88-independent pathway. Considering that endothelial dysfunction is pivotal in the development of sepsis and kidney injury, we hypothesize that the identified molecules might represent a future therapeutic strategy to shield the renal endothelial compartment and promote kidney repair. FJ

ACKNOWLEDGMENTS

This study was supported by University of Bari Aldo Moro, the Italian Ministry of Health (Ricerca Finalizzata 2009 to G.C. and GR-2011-02351027 2011–2012 to G.C.). L.G. was supported by a Regional Strategic Grant, Apulia Region (PSR 094). A.G. and L.G. contributed equally to this work as senior authors. The authors declare no conflicts of interest.

AUTHOR CONTRIBUTIONS

F. Sallustio planned the research, coordinated the study, and drafted the manuscript; A. Stasi designed and performed most experiments, analyzed the respective data, and drafted the manuscript; C. Curci carried out the *in vitro* experiments regarding Western blot and real time-PCR and assisted in manuscript preparation; C. Divella participated in the immunolabeling and confocal microscopy of renal sections and contributed to data analysis; A. Picerno, R. Franzin, and G. De Palma participated in the design of the study and assisted *in vitro* experiments; M. Rutigliano performed isolation and characterization of ARPCs from human renal tissue; G. Lucarelli and M. Battaglia contributed to surgical procedures and revised the manuscript; F. Staffieri and A. Crovace carried out all surgical procedures of the animal model and helped to revise the manuscript; G. Castellano provided new analytic tools, participated in the coordination of the study, and critically revised the manuscript; G. B. Pertosa performed ELISA assays; G. B. Pertosa and A. Gallone participated in the coordination of the study and assisted in manuscript preparation; F. Sallustio, A. Gallone, and L. Gesualdo designed and supervised the research and drafted the manuscript; and all authors read and approved the final manuscript.

REFERENCES

1. Zarjou, A., and Agarwal, A. (2011) Sepsis and acute kidney injury. *J. Am. Soc. Nephrol.* **22**, 999–1006
2. Fiorentino, M., Tohme, F. A., Wang, S., Murugan, R., Angus, D. C., and Kellum, J. A. (2018) Long-term survival in patients with septic acute kidney injury is strongly influenced by renal recovery. *PLoS One* **13**, e0198269
3. Castellano, G., Stasi, A., Intini, A., Gigante, M., Di Palma, A. M., Divella, C., Netti, G. S., Prattichizzo, C., Pontrelli, P., Crovace, A., Staffieri, F., Fiaccadori, E., Brienza, N., Grandaliano, G., Pertosa, G., and Gesualdo, L. (2014) Endothelial dysfunction and renal fibrosis in endotoxemia-induced oliguric kidney injury: possible role of LPS-binding protein. *Crit. Care* **18**, 520
4. Stasi, A., Intini, A., Divella, C., Franzin, R., Montemurno, E., Grandaliano, G., Ronco, C., Fiaccadori, E., Pertosa, G. B., Gesualdo, L., and Castellano, G. (2017) Emerging role of Lipopolysaccharide binding protein in sepsis-induced acute kidney injury. *Nephrol. Dial. Transplant.* **32**, 24–31
5. Gomez, H., Ince, C., De Backer, D., Pickkers, P., Payen, D., Hotchkiss, J., and Kellum, J. A. (2014) A unified theory of sepsis-induced acute kidney injury: inflammation, microcirculatory dysfunction, bioenergetics, and the tubular cell adaptation to injury. *Shock* **41**, 3–11
6. Patschan, D., Patschan, S., and Müller, G. A. (2011) Endothelial progenitor cells in acute ischemic kidney injury: strategies for increasing the cells' renoprotective competence. *Int. J. Nephrol.* **2011**, 828369
7. Wu, L., Gokden, N., and Mayeux, P. R. (2007) Evidence for the role of reactive nitrogen species in polymicrobial sepsis-induced renal peritubular capillary dysfunction and tubular injury. *J. Am. Soc. Nephrol.* **18**, 1807–1815
8. Guerrot, D., Dussaule, J. C., Kavvadas, P., Boffa, J. J., Chadjichristos, C. E., and Chatziantoniou, C. (2012) Progression of renal fibrosis: the underestimated role of endothelial alterations. *Fibrogenesis Tissue Repair* **5** (Suppl 1), S15
9. Echeverría, C., Montorfano, I., Hermosilla, T., Armisén, R., Velásquez, L. A., Cabello-Verrugio, C., Varela, D., and Simon, F. (2014) Endotoxin induces fibrosis in vascular endothelial cells through a mechanism dependent on transient receptor protein melastatin 7 activity. *PLoS One* **9**, e94146
10. Schrier, R. W., and Wang, W. (2004) Acute renal failure and sepsis. *N. Engl. J. Med.* **351**, 159–169
11. Dauphinee, S. M., and Karsan, A. (2006) Lipopolysaccharide signaling in endothelial cells. *Lab. Invest.* **86**, 9–22
12. Lerolle, N., Nochy, D., Guérot, E., Bruneval, P., Fagon, J. Y., Diehl, J. L., and Hill, G. (2010) Histopathology of septic shock induced acute kidney injury: apoptosis and leukocytic infiltration. *Intensive Care Med.* **36**, 471–478
13. Lu, Y. C., Yeh, W. C., and Ohashi, P. S. (2008) LPS/TLR4 signal transduction pathway. *Cytokine* **42**, 145–151
14. Park, B. S., and Lee, J. O. (2013) Recognition of lipopolysaccharide pattern by TLR4 complexes. *Exp. Mol. Med.* **45**, e66
15. Peri, F., Piazza, M., Calabrese, V., Damore, G., and Cighetti, R. (2010) Exploring the LPS/TLR4 signal pathway with small molecules. *Biochem. Soc. Trans.* **38**, 1390–1395
16. Usui, M., Hanamura, N., Hayashi, T., Kawarada, Y., and Suzuki, K. (1998) Molecular cloning, expression and tissue distribution of canine lipopolysaccharide (LPS)-binding protein. *Biochim. Biophys. Acta* **1397**, 202–212
17. Wang, S. C., Klein, R. D., Wahl, W. L., Alarcon, W. H., Garg, R. J., Remick, D. G., and Su, G. L. (1998) Tissue coexpression of LBP and CD14 mRNA in a mouse model of sepsis. *J. Surg. Res.* **76**, 67–73

18. Sallustio, F., Curci, C., Aloisi, A., Toma, C. C., Marulli, E., Serino, G., Cox, S. N., De Palma, G., Stasi, A., Divella, C., Rinaldi, R., and Schena, F. P. (2017) Inhibin-A and decorin secreted by human adult renal stem/progenitor cells through the TLR2 engagement induce renal tubular cell regeneration. *Sci. Rep.* **7**, 8225
19. Sallustio, F., De Benedictis, L., Castellano, G., Zaza, G., Loverre, A., Costantino, V., Grandaliano, G., and Schena, F. P. (2010) TLR2 plays a role in the activation of human resident renal stem/progenitor cells. *FASEB J.* **24**, 514–525
20. Sallustio, F., Serino, G., and Schena, F. P. (2015) Potential reparative role of resident adult renal stem/progenitor cells in acute kidney injury. *Biores. Open Access* **4**, 326–333
21. Bussolati, B., and Camussi, G. (2015) Therapeutic use of human renal progenitor cells for kidney regeneration. *Nat. Rev. Nephrol.* **11**, 695–706
22. Lazzeri, E., Romagnani, P., and Lasagni, L. (2015) Stem cell therapy for kidney disease. *Expert Opin. Biol. Ther.* **15**, 1455–1468
23. Lazzeri, E., Angelotti, M. L., Peired, A., Conte, C., Marschner, J. A., Maggi, L., Mazzinghi, B., Lombardi, D., Melica, M. E., Nardi, S., Ronconi, E., Sisti, A., Antonelli, G., Becherucci, F., De Chiara, L., Guevara, R. R., Burger, A., Schaefer, B., Annunziato, F., Anders, H.-J., Lasagni, L., and Romagnani, P. (2018) Endocycle-related tubular cell hypertrophy and progenitor proliferation recover renal function after acute kidney injury. *Nat. Commun.* **9**, 1344
24. Sallustio, F., Serino, G., Costantino, V., Curci, C., Cox, S. N., De Palma, G., and Schena, F. P. (2013) miR-1915 and miR-1225-5p regulate the expression of CD133, PAX2 and TLR2 in adult renal progenitor cells. *PLoS One* **8**, e68296; erratum: 10, e0128258
25. Boca, S.M., and Leek, J.T. (2018) A direct approach to estimating false discovery rates conditional on covariates [E-pub ahead of print]. *PeerJ.* 10.7717/peerj.6035
26. Curci, C., Castellano, G., Stasi, A., Divella, C., Loverre, A., Gigante, M., Simone, S., Cariello, M., Montinaro, V., Lucarelli, G., Ditonno, P., Battaglia, M., Crovace, A., Staffieri, F., Oortwijn, B., van Amersfoort, E., Gesualdo, L., and Grandaliano, G. (2014) Endothelial-to-mesenchymal transition and renal fibrosis in ischaemia/reperfusion injury are mediated by complement anaphylatoxins and Akt pathway. *Nephrol. Dial. Transplant.* **29**, 799–808
27. Basile, D. P., Friedrich, J. L., Spahic, J., Knipe, N., Mang, H., Leonard, E. C., Changizi-Ashtiyani, S., Bacallao, R. L., Molitoris, B. A., and Sutton, T. A. (2011) Impaired endothelial proliferation and mesenchymal transition contribute to vascular rarefaction following acute kidney injury. *Am. J. Physiol. Renal Physiol.* **300**, F721–F733
28. Zeisberg, E. M., Potenta, S. E., Sugimoto, H., Zeisberg, M., and Kalluri, R. (2008) Fibroblasts in kidney fibrosis emerge via endothelial-to-mesenchymal transition. *J. Am. Soc. Nephrol.* **19**, 2282–2287
29. Zeisberg, M., and Neilson, E. G. (2010) Mechanisms of tubulointerstitial fibrosis. *J. Am. Soc. Nephrol.* **21**, 1819–1834
30. Zeisberg, E. M., Tarnavski, O., Zeisberg, M., Dorfman, A. L., McMullen, J. R., Gustafsson, E., Chandraker, A., Yuan, X., Pu, W. T., Roberts, A. B., Neilson, E. G., Sayegh, M. H., Izumo, S., and Kalluri, R. (2007) Endothelial-to-mesenchymal transition contributes to cardiac fibrosis. *Nat. Med.* **13**, 952–961
31. Kizu, A., Medici, D., and Kalluri, R. (2009) Endothelial-mesenchymal transition as a novel mechanism for generating myofibroblasts during diabetic nephropathy. *Am. J. Pathol.* **175**, 1371–1373
32. Echeverría, C., Montorfano, I., Sarmiento, D., Becerra, A., Nuñez-Villena, F., Figueroa, X. F., Cabello-Verrugio, C., Elorza, A. A., Riedel, C., and Simon, F. (2013) Lipopolysaccharide induces a fibrotic-like phenotype in endothelial cells. *J. Cell. Mol. Med.* **17**, 800–814
33. Martin, L., van Meegern, A., Doemming, S., and Schuerholz, T. (2015) Antimicrobial peptides in human sepsis. *Front. Immunol.* **6**, 404
34. Linge, H. M., Collin, M., Nordenfelt, P., Mörgelin, M., Malmsten, M., and Egesten, A. (2008) The human CXC chemokine granulocyte chemotactic protein 2 (GCP-2)/CXCL6 possesses membrane-disrupting properties and is antibacterial. *Antimicrob. Agents Chemother.* **52**, 2599–2607
35. Besnard, A. G., Struyf, S., Guabiraba, R., Fauconnier, L., Rouxel, N., Proost, P., Uyttenhove, C., Van Snick, J., Couillin, I., and Ryffel, B. (2013) CXCL6 antibody neutralization prevents lung inflammation and fibrosis in mice in the bleomycin model. *J. Leukoc. Biol.* **94**, 1317–1323
36. Gijsbers, K., Gouwy, M., Struyf, S., Wuyts, A., Proost, P., Opdenakker, G., Penninckx, F., Ectors, N., Geboes, K., and Van Damme, J. (2005) GCP-2/CXCL6 synergizes with other endothelial cell-derived chemokines in neutrophil mobilization and is associated with angiogenesis in gastrointestinal tumors. *Exp. Cell Res.* **303**, 331–342
37. Uhlar, C. M., and Whitehead, A. S. (1999) Serum amyloid A, the major vertebrate acute-phase reactant. *Eur. J. Biochem.* **265**, 501–523
38. Sipe, J. (1999) Revised nomenclature for serum amyloid A (SAA). Nomenclature Committee of the International Society of Amyloidosis. Part 2. *Amyloid* **6**, 67–70
39. Kushner, I. (1982) The phenomenon of the acute phase response. *Ann. N. Y. Acad. Sci.* **389**, 39–48
40. Kisilevsky, R., and Manley, P. N. (2012) Acute-phase serum amyloid A: perspectives on its physiological and pathological roles. *Amyloid* **19**, 5–14
41. Meek, R. L., Eriksen, N., and Benditt, E. P. (1989) Serum amyloid A in the mouse. Sites of uptake and mRNA expression. *Am. J. Pathol.* **135**, 411–419
42. Olsen, H. G., Skovgaard, K., Nielsen, O. L., Leifsson, P. S., Jensen, H. E., Iburg, T., and Heegaard, P. M. (2013) Organization and biology of the porcine serum amyloid A (SAA) gene cluster: isoform specific responses to bacterial infection. *PLoS One* **8**, e76695
43. Elsbach, P. (1998) The bactericidal/permeability-increasing protein (BPI) in antibacterial host defense. *J. Leukoc. Biol.* **64**, 14–18
44. Gorr, S.-U., Hirt, H., and Nandula, S. R. (2015) The salivary protein PSP/Bpifa2 protects against intestinal inflammation. *FASEB J.* **29**, LB684
45. Bingle, C. D., and Craven, C. J. (2002) PLUNC: a novel family of candidate host defence proteins expressed in the upper airways and nasopharynx. *Hum. Mol. Genet.* **11**, 937–943
46. Weiss, J., Elsbach, P., Shu, C., Castillo, J., Grinna, L., Horwitz, A., and Theofan, G. (1992) Human bactericidal/permeability-increasing protein and a recombinant NH2-terminal fragment cause killing of serum-resistant gram-negative bacteria in whole blood and inhibit tumor necrosis factor release induced by the bacteria. *J. Clin. Invest.* **90**, 1122–1130
47. Kota, S. K., Pernicone, E., Leaf, D. E., Stillman, I. E., Waikar, S. S., and Kota, S. B. (2017) BPI fold-containing family a member 2/parotid secretory protein is an early biomarker of AKI. *J. Am. Soc. Nephrol.* **28**, 3473–3478
48. Tanimura, N., Saitoh, S., Matsumoto, F., Akashi-Takamura, S., and Miyake, K. (2008) Roles for LPS-dependent interaction and relocation of TLR4 and TRAM in TRIF-signaling. *Biochem. Biophys. Res. Commun.* **368**, 94–99
49. Tarassishin, L., Bauman, A., Suh, H. S., and Lee, S. C. (2013) Anti-viral and anti-inflammatory mechanisms of the innate immune transcription factor interferon regulatory factor 3: relevance to human CNS diseases. *J. Neuroimmune Pharmacol.* **8**, 132–144
50. Li, X., Tupper, J. C., Bannerman, D. D., Winn, R. K., Rhodes, C. J., and Harlan, J. M. (2003) Phosphoinositide 3 kinase mediates toll-like receptor 4-induced activation of NF-kappa B in endothelial cells. *Infect. Immun.* **71**, 4414–4420
51. Vivarelli, M. S., McDonald, D., Miller, M., Cusson, N., Kelliher, M., and Geha, R. S. (2004) RIP links TLR4 to Akt and is essential for cell survival in response to LPS stimulation. *J. Exp. Med.* **200**, 399–404
52. Ojaniemi, M., Glumoff, V., Harju, K., Liljeroos, M., Vuori, K., and Hallman, M. (2003) Phosphatidylinositol 3-kinase is involved in toll-like receptor 4-mediated cytokine expression in mouse macrophages. *Eur. J. Immunol.* **33**, 597–605

Received for publication February 4, 2019.
Accepted for publication June 4, 2019.